Science of the Total Environment 934 (2024) 173219

Contents lists available at ScienceDirect

Science of the Total Environment

journal homepage: www.elsevier.com/locate/scitotenv

Role of macroalgal forests within Mediterranean shallow bays in blue carbon storage

Uxue Moreda [a], Inés Mazarrasa [a,b], Emma Cebrian [a], Joeri Kaal [c], Aurora M. Ricart [d], Eduard Serrano [a], Oscar Serrano [a,*]

[a] Centre d'Estudis Avançats de Blanes, Consejo Superior de Investigaciones Científicas (CEAB-CSIC), Blanes, Spain
[b] Instituto de Hidráulica Ambiental de la Universidad de Cantabria (IHCantabria), Santander, Spain
[c] Pyrolyscience, 15707 Santiago de Compostela, Spain
[d] Institut de Ciències del Mar, Consejo Superior de Investigaciones Científicas (ICM-CSIC), Barcelona, Spain

HIGHLIGHTS

- Scarcity of empirical evidence demonstrating long-term storage of macroalgae carbon
- Stable isotopes and pyrolysis showcased macroalgae carbon preservation in sediments
- Burial rates of macroalgae carbon up to 4-fold higher than previous estimates
- Storage of macroalgae carbon supports their inclusion in blue carbon frameworks.

GRAPHICAL ABSTRACT

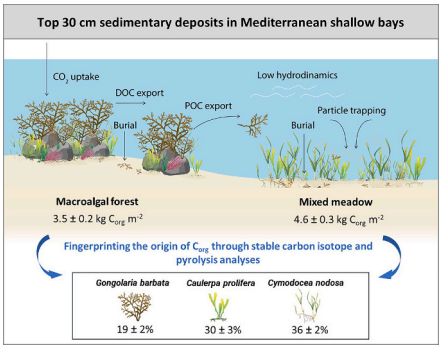

ARTICLE INFO

Editor: Ouyang Wei

Keywords:
Organic carbon
Seaweed
Climate change mitigation
Fingerprint
Pyrolysis-GC–MS
Conservation

ABSTRACT

Although seaweeds rank among the most productive vegetated habitats globally, their inclusion within Blue Carbon frameworks is at its onset, partially because they usually grow in rocky substrates and their organic carbon (C_{org}) is mostly exported and stored beyond their habitat and thus, demonstrating its long-term storage is challenging. Here, we studied the sedimentary C_{org} storage in macroalgal forests dominated by *Gongolaria barbata* and in adjacent seagrass *Cymodocea nodosa* mixed with *Caulerpa prolifera* algae meadows, and bare sand habitats in Mediterranean shallow coastal embayments. We characterized the biogeochemistry of top 30 cm sedimentary deposits, including sediment grain-size, organic matter and C_{org} contents, C_{org} burial rates and the provenance of sedimentary C_{org} throughout stable carbon isotopes ($\delta^{13}C_{org}$) and pyrolysis analyses. Sediment C_{org} stocks and burial rates (since 1950) in *G. barbata* forests (mean ± SE, 3.5 ± 0.2 kg C_{org} m^{-2} accumulated at 15.5

Abbreviations: C_{org}, Organic Carbon; $\delta^{13}C_{org}$, Stable Carbon Isotopes; BCE, Blue Carbon Ecosystems; POC, Particulate Organic Carbon; DOC, Dissolved Organic Carbon; GHG, Greenhouse Gases; Py-GC–MS, Pyrolysis-Gas Chromatography–Mass Spectrometry; THM-GC–MS, Thermally Assisted Hydrolysis and Methylation; DW, Dry Weight; DBD, Dry Bulk Density; MAR, Mass Accumulation Rates; SAR, Sediment Accumulation Rate; OM, Organic Matter Concentration; LOI, Loss on Ignition; GLMM, Generalized Linear Mixed Models; TQPA, Total Quantified Peak Area; EF, Enrichment Factor; N-compounds, Compounds with Nitrogen; FAMEs, Fatty Acid Methyl Esters.

* Corresponding author.
E-mail address: oserrano@ceab.csic.es (O. Serrano).

https://doi.org/10.1016/j.scitotenv.2024.173219
Received 28 February 2024; Received in revised form 8 May 2024; Accepted 11 May 2024
Available online 14 May 2024

± 1.6 g C_{org} m^{-2} y^{-1}) fall within the range of those reported for traditional Blue Carbon Ecosystems. Although the main species contributing to sedimentary C_{org} stocks in all vegetated habitats examined was *C. nodosa* (36 ± 2 %), macroalgae contributed 49 % (19 ± 2 % by *G. barbata* and 30 ± 3 % by *C. prolifera*) based on isotope mixing model results. Analytical pyrolysis confirmed the presence of macroalgae-derived compounds in the sediments, including N-compounds and α-tocopherol linked to *G. barbata* and *C. prolifera*, respectively. The sedimentary C_{org} burial rate linked to macroalgae within the macroalgal forests examined ranged from 5.4 to 9.5 g C_{org} m^{-2} y^{-1} (7.4 ± 2 g C_{org} m^{-2} y^{-1}). This study provides empirical evidence for the long-term (~70 years) sequestration of macroalgae-derived C_{org} within and beyond seaweed forests in Mediterranean shallow coastal embayments and thereby, supports the inclusion of macroalgae in Blue Carbon frameworks.

1. Introduction

Over the past decades, Blue Carbon Ecosystems (BCE), in particular mangroves, tidal marshes, and seagrass meadows, have been identified as natural carbon sinks thanks to their capacity to accumulate organic carbon (C_{org}) and to store it in the long-term (Smith, 1981; Mcleod et al., 2011; Mateo et al., 1997). The historic and current losses of BCE due to global change impacts claim for their conservation and restoration as effective strategies to mitigate climate change, as they would avoid greenhouse gas emissions derived from ecosystem degradation and increase CO_2 sequestration (Gattuso et al., 2018; Macreadie et al., 2021) while enhancing other valuable ecosystem services (e.g., fisheries support, coastal protection and biodiversity) key for climate change adaptation, food security, and human wellbeing (McLeod et al., 2011; Himes-Cornell et al., 2018; Lovelock and Reef, 2020).

The C_{org} storage capacity of BCE results from their high primary productivity (Smith, 1981) and the accumulation of autochthonous C_{org} in the biomass and soil. BCE also accumulate C_{org} from external sources (allochthonous C_{org}), such as terrestrial biomass, seston or decaying organic matter from other marine macrophytes through the sedimentation of particles from the water column (Kennedy et al., 2010). The canopies (aboveground biomass) of BCE contribute to attenuate water flow and enhance particle sedimentation, whereas the roots and rhizomes stabilize the sediments and prevent resuspension (Gruber and Kemp, 2010; Samosorn et al., 2018). As a consequence, BCE soils are usually enriched in silt and clay (Herkül and Kotta, 2009), which facilitate the preservation of C_{org} by limiting oxygen availability and by physically protecting (through adsorption forces) organic particles from the action of decomposers (Keil et al., 1994; Burdige, 2007).

Recently, the inclusion of other marine ecosystems, such as seaweed in Blue Carbon frameworks is being discussed within the scientific and policy areas (IPCC; Claes et al., 2022). Seaweed-dominated habitats rank among the most productive vegetated habitats globally, with likely higher contribution to the ocean carbon budget than traditional BCE (Duarte et al., 2022). Most macroalgae species grow in rocky environments and therefore, they are unlikely to develop sedimentary C_{org} deposits that are found underneath traditional BCEs (Pessarrodona et al., 2023). Yet, macroalgae thallus can be detached or fragmented, transported and accumulated within seaweed forest and beyond (Handayani et al., 2022), and the highly recalcitrant compounds present in their biomass contribute to the long-term persistence of macroalgae-derived particulate and dissolved C_{org} (POC and DOC, respectively) in the sediments and in the water column (Trevathan-Tackett et al., 2015). Although the potential of macroalgae as BCE is undeniable, empirical evidence of macroalgae-derived C_{org} export and long-term preservation is still limited, holding back their inclusion into Blue Carbon policy frameworks. There are few studies exploring detritus transport pathways via modelling and remote sensing (e.g., Ager et al., 2023; Queirós et al., 2023), including reports on the occurrence of macroalgal biomass in near-shore and deep-sea surface sediments (Erlania et al., 2023; Arina et al., 2023; Ortega et al., 2020; Queirós et al., 2019). However, the quantitative evaluation of carbon fluxes in macroalgal ecosystems is complex owing to the large spatial and temporal scales involved.

The inclusion of macroalgae within national carbon inventories requires determining the provenance of C_{org} accumulated within the sediment together with the identification of donor habitats where conservation and/or restoration actions occurred. Most studies have used carbon isotopic signatures to fingerprint the origin of sedimentary C_{org}, but the accuracy of this method is frequently insufficient (Geraldi et al., 2019). Although emerging techniques such as compound-specific isotopes, biomarkers, and environmental DNA (eDNA) are qualitative or semiquantitative and thereby, provide limited information of the pathways beyond the carbon cycle, they could bring valuable insights to identify the provenance of sedimentary C_{org} (Evershed et al., 2007; Derrien et al., 2017; Reef et al., 2017). In particular, Kaal et al. (2020) evidenced that analytical pyrolysis techniques (pyrolysis-gas chromatography–mass spectrometry; Py-GC–MS; Van de Meent et al., 1980; and thermally assisted hydrolysis and methylation; THM-GC–MS; Pulchan et al., 1997) can be used to identify source-specific macromolecular C_{org} constituents within coastal sediments. However, the application of analytical pyrolysis techniques in Blue Carbon research is at its onset and has never been used before to detect macroalgae-derived organic matter in marine sediments.

Similar to traditional BCE, seaweed-dominated habitats are also under threat at a global scale (Filbee-Dexter and Wernberg, 2018; Pessarrodona et al., 2021). In the Mediterranean Sea, macroalgal forests growing in shallow sheltered bays are especially vulnerable to degradation due to the appeal of these environments for tourism and urban development (Thibaut et al., 2005). These habitats of high ecological value are classified as "*Large shallow inlets and bays, code 1160*" within the Natura 2000 framework and protected under the European Habitats Directive. The vegetated benthic communities that develop in these habitats are characterized by harbouring highly complex macroalgal forests with structured canopy forming species of *Cystoseira* sensu lato (including *Ericaria*, *Gongolaria* and *Cystoseira* genera; Novoa and Guiry, 2019), that grow on rocky and detrital substrates often adjacent or within seagrass *Posidonia oceanica*, *Cymodocea nodosa* and *Zostera marina* meadows and/or rizhophytic *Caulerpa prolifera* macroalgae. Even though previous studies have demonstrated the relevance of macroalgal forest in Mediterranean shallow embayments as biodiversity hotspots (Galobart et al., 2023), data on carbon fluxes associated with macroalgal forests is scarce, and their role as carbon sinks remains to be explored.

The aim of this study is to assess the origin and magnitude of sedimentary C_{org} stores in vegetated Mediterranean shallow water bays and to explore the contribution of macroalgal forests to long-term C_{org} burial within and beyond their habitats. For this purpose, we characterized the sediment C_{org} deposits (e.g., magnitude, accumulation rates and their origin) across two macroalgal forests dominated by *Gongolaria barbata*, and also in adjacent habitats formed by a mixed *C. nodosa* and *C. prolifera* meadow, and in bare sand. We used a multi-proxy approach combining isotopic analyses along with cutting-edge pyrolysis techniques to fingerprint the provenance of sedimentary C_{org}.

2. Materials and methods

2.1. Study site

This study was conducted in two shallow sheltered bays at Menorca

(Balearic Islands), in the North-Western Mediterranean Sea (Fig. 1). The two study sites, Cala Rotja (40.0348° N, 4.1363° E) and Cala Teulera (39.8780° N, 4.3077° E), are found in the shallow and protected bays of Fornells and Maó, respectively. These two sites hold well-preserved marine ecosystems typical of Mediterranean shallow bays, formed by seagrass meadows and macroalgal forest dominated by *G. barbata*.

2.2. Sampling procedures

Sampling at Cala Rotja was conducted in a *G. barbata* forest (from here on referred as "forest I") and in an adjacent mixed meadow formed by the seagrass *C. nodosa* and the macroalgae *C. prolifera* (referred as "mixed meadow"). Sampling at Cala Teulera was conducted in a *G. barbata* forest (referred as "forest II") and in an adjacent unvegetated sand area (referred as "bare sand") (Fig. 1). In both study sites macroalgal forests were dominated by *G. barbata* fronds growing on top of pebbles and stones sitting on sandy substrates along the shoreline. *C. nodosa* was more abundant in the *G. barbata* forest from Cala Teulera, whereas *C. prolifera* was more abundant in the *G. barbata* forest from Cala Rotja. In the mixed meadow, *C. nodosa* and *C. prolifera* inhabited a soft bottom area further away (40 m) from the shoreline. The bare sand habitat consisted in a >100 m^2 patch of sand next to the shoreline. Sampling was conducted at water depths ranging from 0.5 to 1.5 m.

Three sediment cores were sampled in each habitat by manually hammering PVC tubes (100 cm long, 6.5 cm internal diameter). The cores were sealed at both ends and kept refrigerated at 4 °C until further processing. Sediment compression while coring was measured and used to correct sediment compaction assuming that sediment compression was linear (Serrano et al., 2014). Tissue samples of the most abundant macrophytes present at the study sites (*G. barbata*, *C. prolifera* and *C. nodosa*) were collected for further analyses.

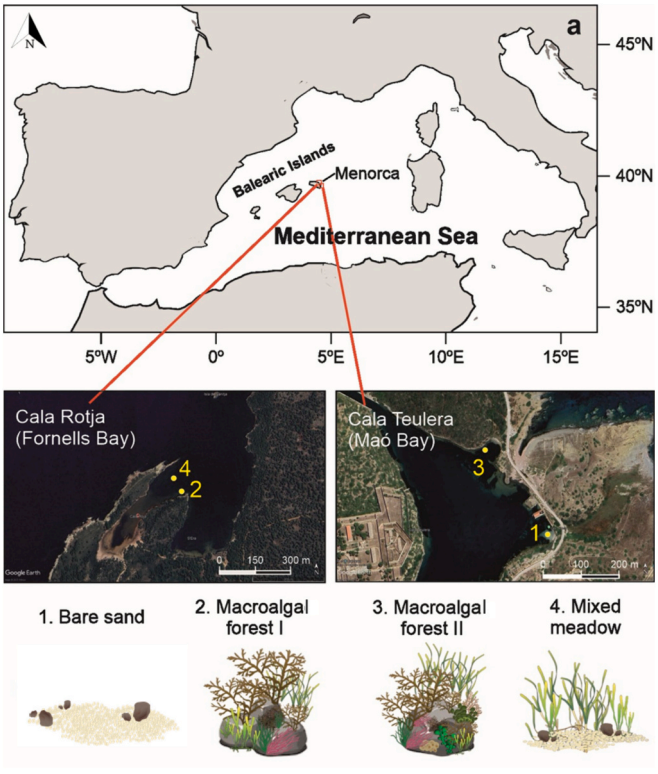

Fig. 1. Sampling sites in Menorca (Balearic Islands, Mediterranean Sea): Cala Rotja in Fornells Bay and Cala Teulera in Maó Bay. Three replicate sediment cores were sampled in four habitats: two macroalgal forests of *Gongolaria barbata*, a mixed meadow of *Cymodocea nodosa* and *Caulerpa prolifera*, and a bare sand area (adapted from Galobart et al., 2023).

2.3. Laboratory procedures and biogeochemical analyses

The PVC tubes were cut lengthwise and opened to slice the sediment cores at 1 cm intervals for the upper 20 cm depth, at 3 cm intervals for 20 to 50 cm depth, at 5 cm intervals for 50 to 60 cm depth, and at 10 cm intervals for the remaining of the cores below 60 cm depth. A subsample (approximately ¾ of the volume of each slice) was obtained by quartering, and dried at 60 °C until constant weight for sediment grain-size, organic matter and C_{org} element and isotopic composition, whereas the remaining sample and the tissue samples of macrophytes were freeze dried prior to radioisotope and pyrolysis analyses. Oven- and freeze-dried samples from each sediment slice were weighed (dry weight, DW), and the weights were pooled to calculate the sediment dry bulk density by dividing the DW by the fresh volume (DBD, in g DW cm^{-3}).

Radioisotope analyses (^{210}Pb, ^{226}Ra, and ^{137}Cs analysis) were run in alternate slices within the top 30 cm of one replicate core from both macroalgal forests I and II by direct gamma using an Ortec HPGe GWL series well-type coaxial low background intrinsic germanium detectors (Appleby et al., 1986). The ^{226}Ra data was used to determine the excess of concentrations (supported ^{210}Pb). The Constant Flux and Constant Sedimentation model (CF:CS; Krishnaswamy et al., 1971) was fitted to the excess ^{210}Pb concentrations (i.e., after subtracting the supported ^{210}Pb concentrations) to determine sediment mass accumulation rates (MAR, g cm^{-2} y^{-1}), sediment accumulation rates (SAR, cm y^{-1}) and the sediment age along the depth profile (Appleby et al., 1992). The ^{137}Cs data was used as an absolute age marker to refine the chronological model obtained.

Sediment grain-size was analysed in bulk samples from all sediment slices using a Mastersizer 2000 laser-diffraction particle analyser after digestion of ~10 g of sample with 30 % hydrogen peroxide to digest the organic matter. Particle sizes (%) were classified following the Udden-Wentworth grain size scale: <63 μm in diameter, silt and clay; 63–150 μm, very fine sand; 150–250 μm, fine sand; 250–500 μm, medium sand; 250–1000 μm, coarse sand; and >1000 μm, very coarse sand and gravel. The rest of the sample was milled in a ball mill grinder and divided for subsequent analyses.

The sediment organic matter concentration (OM, in %DW) was determined in all milled sediment samples (~4 g of dried sample) through the loss on ignition technique (LOI), as the weight loss after combustion at 450 °C for 4 h (Heiri et al., 2001). Sediment C_{org} (in % DW) and stable carbon isotopes ($\delta^{13}C_{org}$) were measured in selected sediment slices along all cores (at 0–1, 4–5, 9–10, 19–20, 29–32, and 38–41 cm compressed sediment depth) and in macrophyte tissue samples using an Elemental Analyser - Isotope Ratio Mass Spectrometry (EA-IRMS). About 1 g of ground sample was acidified with 4 % HCl to remove inorganic carbon, centrifuged (3400 rpm, for 5 min), and the supernatant with acid residues was carefully removed with a pipette, avoiding resuspension. The sample was then washed with Milli-Q water, centrifuged and the supernatant removed. The residual samples were re-dried and then encapsulated in tin capsules prior to analyses. The C_{org} content was calculated for the bulk (pre-acidified) samples. Macrophyte samples returned a negative test for the presence of carbonates after adding 10 % HCl and therefore, were not acidified prior to $\%C_{org}$ and $\delta^{13}C_{org}$ analyses. Carbon isotope ratios are expressed as δ values in parts per thousand (‰) relative to the Vienna Pee Dee Belemnite standard.

The $\%C_{org}$ in the remaining sediment samples was estimated by applying the linear regression obtained from the relationship between % OM and $\%C_{org}$ in the samples were both analyses were conducted ($R^2 = 0.95$, $N = 68$, see Supplementary Fig. S1). The C_{org} density (g C_{org} cm^{-3}) for each sediment slice was calculated by multiplying C_{org} (%DW) and sediment DBD (g DW cm^{-3}), and dividing by 100. The cumulative C_{org} stocks (kg C_{org} cm^{-2}) for the top 30 cm of sediment (decompressed) in each core were estimated as the cumulative mass of C_{org} density up to 30 cm depth. The C_{org} burial rates in the macroalgal forests were estimated for the period between 1950 and 2021 by multiplying MAR and $\%C_{org}$, and dividing by 100.

All the statistical analyses were run in R version 4.3.1 (R Core Team, 2023). Generalized Linear Mixed Models (GLMM, family = Gamma; package lme4; Bates et al., 2015) were performed to assess differences in sediment biogeochemical properties (DBD, %C_{org}, C_{org} density, C_{org} stock in top 30 cm, $\delta^{13}C$ signatures and sediment grain size fractions) across the four habitats examined. GLMM were used instead of ANOVA to account for the lack of independency of the data collected along sediment depth profiles. All the data were square-root transformed and standardized to 30 cm depth (decompressed) prior to statistical analyses. The type of habitat (bare sand, macroalgal forests I and II, and mixed meadow) was included as a fixed factor, whereas sediment depth (cm along sediment cores) and study site (Cala Teulera and Cala Rotja) were included as random factors in all statistical models. Besides, $\delta^{13}C$ signatures variations along depth (fixed factor, levels: 1, 5, 10, 20, and 30 cm compressed) were tested for the different habitats, and study site was included as a random factor. GLMM were also performed to assess differences in C_{org} burial rates between macroalgal forests I and II (habitat included as a fixed factor, and sediment depth included as a random factor). Pearson correlation analyses were run to assess the influence of silt and clay content (<63 μm) on C_{org} storage.

A Stable Isotope Mixing Model was applied to all the cores along sediment depth (1, 5, 10, 20, and 30 cm compressed) to assess the contribution of potential C_{org} sources to the sediment C_{org} stocks using simmr package version 0.5.1 in R (Govan and Parnell, 2019), with one isotope as tracer ($\delta^{13}C_{org}$). Four potential sources were considered in the model: the three main macrophyte species present in the study areas (*G. barbata*, *C. prolifera* and *C. nodosa*) and seston (i.e., the particulate matter from the surface water). Since the riverine inputs in the Balearic Islands are negligible, seston is assumed to represent mostly phytoplankton-derived C_{org} (Papadimitriou et al., 2005; Dauby, 1989). The mean and standard deviation of isotopic signatures $\delta^{13}C_{org}$ for *G. barbata*, *C. prolifera*, *C. nodosa* and seston matter to run the model were obtained from this study and from previous studies conducted in the Balearic Islands and other regions in the Mediterranean Sea (Vizzini et al., 2002; Sarà et al., 2003; Papadimitriou et al., 2005; Fourqurean et al., 2007) (Supplementary Table S1) aiming at embracing spatial and seasonal variability in $\delta^{13}C_{org}$ signatures. The proportion of each source according to the outputs of the mixing model were used to calculate the total contribution of each source to the top 30 cm C_{org} stocks within each habitat and at five sediment depths (1, 5, 10, 20 and 30 cm compressed).

The values for variables DBD, grain size, C_{org} (%DW) and $\delta^{13}C_{org}$ are expressed as mean ± standard error (SE) based on the multiple analyses conducted in the different slices within the top 30 cm of all three replicate cores studied in each habitat. For C_{org} stocks, the error was calculated based on the deviation from the mean value of the three replicate cores studied in each habitat. The values for at different depths are expressed as the mean ± SE of replicate samples. The SE of MAR and SAR was estimated through the CR:CS model, and the standard errors of C_{org} burial were estimated by propagating the errors of MAR and C_{org} stock.

2.3.1. Molecular composition of the organic matter (Py-GC–MS and THM-GC–MS)

Conventional pyrolysis-gas chromatography–mass spectrometry (Py-GC–MS) and thermally assisted hydrolysis and methylation (THM-GC–MS) analyses were carried out in one core per habitat at three selected sediment depths along the top 30 cm (0–1, 14–15 and 29–32 cm), and in the macrophyte samples. Carbonates in freeze dried and ground samples (1 g) of macrophyte and sediments were dissolved by adding aliquots of 4 % HCl until the reaction ceased, after which distilled water was added until 30 mL. The suspension was centrifuged (4000 rpm, 8 min) and the supernatant was carefully removed to avoid resuspension. The residue was rinsed with ultrapure Milli-Q water, centrifuged (4000 rpm for 8 min), and dried at 60 °C for 24 h after removing the supernatant. Pre-treated samples were analysed with a Pyroprobe 5000 (CDS Analytical) coupled to an 8860 GC and 5977B MSD (Agilent Technologies). To perform Py-GC–MS, the digested samples were placed in fire-polished quartz tubes, and pyrolyzed at 650 °C for 20 s. The pyrolyzates were swept from the pyrolysis chamber using the helium carrier gas (1 mL min^{-1}) into the inlet of the GC (at 325 °C, and in split mode 1:10). The GC oven was heated from 80 to 325 °C at a rate of 30 °C min^{-1}, then held isothermal for 3 min. The column used was an HP-5MS. The MS operated in electron ionization mode (70 eV) and in scan mode (50–500 *m/z*). The same instruments were used for THM-GC–MS analyses, but in this case the samples were placed in quartz tubes after which an aliquot of 25 % tetramethyl ammonium hydroxide (TMAH, in water, Sigma ®) was added. The analytical parameters for THM-GC–MS were the same as for Py-GC–MS, except for the GC oven program (from 100 °C with an isothermal hold of 3 min, heating rate 40 °C min^{-1}, final isothermal hold of 3 min) and the split ratio of the GC inlet (1:50).

Products in sediment and macrophyte samples were semi-quantified based on the peak area of one or two dominant *m/z* fragments of each compound, expressed as the relative proportion (%) of the total quantified peak area (TQPA). The enrichment factor (EF) of the compounds in each potential macrophyte source was calculated as the % of a compound divided by the average % value of the compound in all the sources. The sums of compounds with EF > 3 (i.e. marker products and products with high indicator value) in the potential sources were used to estimate their contribution in the sediment samples. Pyrolysis products (molecular compounds) were identified, when possible, based on existing literature and previous studies using the same analytical methodologies. All values are mean ± SE of replicate samples.

3. Results

3.1. Age-depth models and sedimentation rates

Total ^{210}Pb activity in the macroalgal forest I and II dated cores reached equilibrium with ^{226}Ra at 12 and 18 cm depth (compressed), respectively (Supplementary Fig. S2), that correspond to the depths up to where sediment age models could be applied. In both cores, the decrease in unsupported ^{210}Pb concentrations with increasing sediment depth suggests a relatively uniform sedimentation through the period spanned by the ^{210}Pb record, except for the top 3 cm in the macroalgal forest I that could indicate mixing (Supplementary Fig. S2). The maximum ages reached in the macroalgal forests I and II corresponded to year 1956 (at 17 cm decompressed) and 1948 (at 22 cm decompressed), respectively. Average sediment accumulation rates since 1950 were estimated at 0.18 ± 0.04 cm y^{-1} in the macroalgal forest I and at 0.22 ± 0.03 cm y^{-1} in the macroalgal forest II.

3.2. Sediment biogeochemical characteristics

The DBD, %C_{org} content, silt and clay (<63 μm) content, C_{org} stocks and $\delta^{13}C_{org}$ (‰) signatures within the top 30 cm of the sediment cores were significantly different among habitat types (GLMM, $p < 0.001$; Table 1A, Fig. 2, Supplementary Fig. S3 and Table S2).

Within the top 30 cm, bare sand sediments had significantly higher DBD (1.06 ± 0.02 g cm^{-3}; $p < 0.001$) than the other habitats surveyed, whereas DBD in the macroalgal forests (I: 0.96 ± 0.30 g cm^{-3}, and II: 0.67 ± 0.04 g cm^{-3}) were ~ 2-fold higher than in the mixed meadow (0.35 ± 0.01 g cm^{-3}; Table 1A, Fig. 2A and Supplementary Fig. S3). Sediments across the habitats studied were dominated by sands (>63 μm; 73–98 %; Supplementary Fig. S4). However, the contribution of different grain-size fractions differed across the habitats (GLMM, $p < 0.001$; Table 1A), with >2-fold higher silt and clay (<63 μm) content in the mixed meadow (27.0 ± 0.8 %) than in the macroalgal forests I and II (9.0 ± 0.1 and 13.0 ± 0.8 %, respectively), and 15-fold higher than in the bare sand (1.8 ± 0.2 %; Fig. 2B).

Within the top 30 cm, the C_{org} content in the mixed meadow sediments (4.5 ± 0.1 % C_{org}) was >2-fold higher than in macroalgal forests I

Table 1
Results from the Generalized Linear Mixed Models (GLMM), including pairwise post-hoc comparisons. A) Differences in sediment dry bulk density (DBD), organic carbon (%C_{org}), silt and clay content (%), organic carbon stock (C_{org} stock), and stable carbon isotope signatures ($\delta^{13}C_{org}$) within the top 30 cm of the sediment cores among habitats (bare sand, macroalgal forest I and II, and mixed meadow), and differences in sediment C_{org} burial rates since 1950 between macroalgal forests I and II. B) Differences in stable carbon isotope signatures ($\delta^{13}C$) among sediment depths (at 1, 5, 10, 20, and 30 cm compressed) within each habitat type surveyed. Significant values are highlighted in bold.

A

Factor	Variable	χ^2	d.f.	*p*-Value
Habitat	DBD (g DW cm^{-3})	393.77	3	**<0.001**
	Pairwise: Bare > Forest I > Forest II > Mixed meadow			
	C_{org} (%DW)	835.78	3	**<0.001**
	Pairwise: Bare < Forest I = Forest II < Mixed meadow			
	<63 μm (%)	147.56	3	**<0.001**
	Pairwise: Bare < Forest I = Forest II < Mixed meadow			
	C_{org} stock (kg C_{org} m^{-2})	270.03	3	**<0.001**
	Pairwise: Bare < Forest I < Forest II < Mixed meadow			
	$\delta^{13}C_{org}$ (‰)	1161.50	3	**<0.001**
	Pairwise: Bare < Forest I = Forest II = Mixed meadow			
	C_{org} burial rate (g C_{org} m^{-2} y^{-1})	255.32	1	**<0.001**

B

Factor	Variable	Habitat	χ^2	d.f.	p-Value
Depth	$\delta^{13}C_{org}$	Bare	32.68	5	**<0.001**
		Forest I	172.39	4	**<0.001**
		Forest II	64.23	5	**<0.001**
		Meadow	10.50	5	0.062

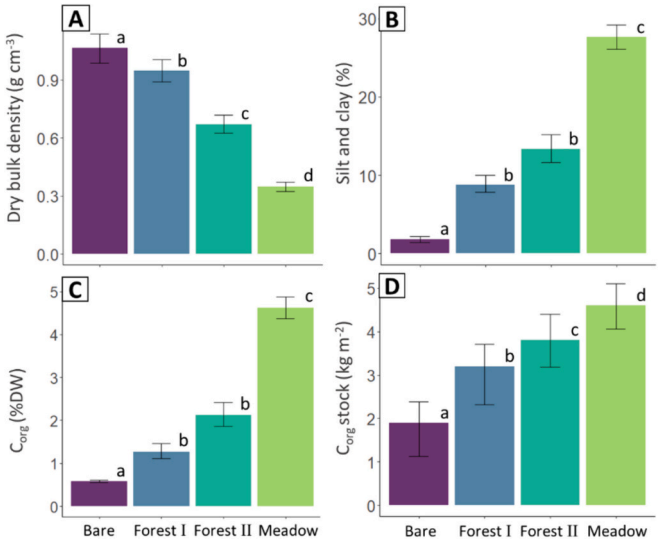

Fig. 2. Average (±SE) values of sediment biogeochemical properties in the top 30 cm of the habitats surveyed (bare sand, macroalgal forests I and II, and mixed meadow): A) dry bulk density (g cm^{-3}); B) silt and clay content (%; <63 μm); C) sediment C_{org} content (%DW); and D) cumulative C_{org} stock (kg C_{org} m^{-2}). Different letters (a, b, c, d) indicate significant differences ($p < 0.001$) among habitats.

and II (1.2 ± 0.7 and 2.1 ± 0.1 % C_{org}, respectively), whereas the bare sand showed the lowest value (0.6 ± 0.01 % C_{org}; $p < 0.001$; Table 1A; Fig. 2C). C_{org} content was positively correlated with silt and clay content in bare, forest II and meadow habitats (R^2 = 0.51, 0.43 and 0.23, respectively), and not correlated in forest I habitat ($R^2 = 0.01$). Sediment C_{org} stocks were also significantly higher in the mixed meadow (4.6 ± 0.3 kg C_{org} m^{-2}) compared to the macroalgal forests I and II (3.2 ± 0.4 and 3.8 ± 0.3 kg C_{org} m^{-2}, respectively; mean of 3.5 ± 0.2 kg C_{org} m^{-2}) and bare sand (1.9 ± 0.4 kg C_{org} m^{-2}; $p < 0.001$; Fig. 2D). Average sediment C_{org} burial rate since 1950 was significantly higher in the macroalgal forest II than in the macroalgal forest I (18.1 ± 2.7 g C_{org} m^{-2} y^{-1} and 12.9 ± 1.6 g C_{org} m^{-2} y^{-1}, respectively; mean of 15.5 ± 1.6 g C_{org} m^{-2} y^{-1}; $p < 0.001$; Table 1A).

3.3. Fingerprinting the origin of organic carbon stores

3.3.1. Pyrolysis-GC–MS

The products detected in both sediments and macrophytes originated from polysaccharides (furans, furaldehydes, cyclopentenones, pyrans and anhydrosugars), nitrogen-containing biopolymers such as protein and chitin (pyrroles, pyridines, cyanobenzenes, indoles and diketopiperazines), polymethylene chain aliphatic compounds (MCC; alkanes, alkenes, fatty acids and phytadienes), products of lignin and lignin-like phenolics (4-vinylphenol, guaiacols and syringols), other phenols (phenol and alkylphenols), aromatic hydrocarbons (benzene and toluene), and other compounds (including benzaldehydes and unidentified compounds) (Supplementary Table S3).

The macrophyte samples considered as potential sources to the sedimentary C_{org} pool produced high proportions of polysaccharide products (>45 % of TQPA). The only macrophyte that produced significant levels of lignin products (4-vinylphenol, guaiacols and syringols) was *C. nodosa* (8.5 %; all other samples < 0.8 %), showing that only this seagrass species contains a significant amount of lignin. Other phenols (phenol and alkylphenols) were also enriched in *C. nodosa* (11.2 %) compared to the other macrophyte species analysed (2.2–6.4 %). The compounds with nitrogen (N-compounds) were more abundant in *C. nodosa* (13.0 %) and *G. barbata* (10.7 %) than in *C. prolifera* (3.2 %), which is indicative of a higher protein content of the former pair. The α-tocopherol (vitamin E) was more abundant in *C. prolifera* (6.5 %).

In the sediment samples, lignin products were most abundant in the macroalgal forest II (4–7 %) and in the mixed meadow (2–3 %), whereas their presence in the bare sand and macroalgal forest I sediments was negligible (≤0.3 %). Polysaccharide contributions varied between 4 and 20 %, without consistent differences among habitats. The N-compounds were abundant in the sediments of the mixed meadow (ranging from 20 to 22 %), depleted in the bare sand (1–7 %), and highly variable in the sediments from the macroalgal forests (5–18 %). The sum of the N-compounds was correlated to organic matter content ($R^2 = 0.72$, $N = 12$; Supplementary Fig. S5), suggesting that organic-rich sediments tend to store N-rich organic matter, in addition to lignin.

Each macrophyte species tested produced markers or indicator compounds with EF > 3 (Supplementary Table S3). Owing to the partial overlapping of these compounds among the reference materials and other putative sources, it was not possible to use them as absolute markers and therefore, the data should be interpreted only in terms of presence/absence rather than quantitatively. Fig. 4 shows the presence of *G. barbata* indicators in the sediments of the mixed meadow, the macroalgal forest II and particularly, within the surface sediments of the macroalgal forest I. *C. prolifera* was likely present in the sediments of the mixed meadow and at 15 cm (compressed) depth in the macroalgal forest I. The cumulative abundance of compounds indicative of *C. nodosa* was much higher than for the other macrophytes explored, which suggests that the seagrass matter was present in all the sediment samples except for the bare sand. In addition to *C. nodosa*, the presence of seagrass *P. oceanica* debris can be inferred for several samples, based on the high abundance of phenol (35–45 % of) in the deeper layers of the macroalgal forest II core, since *P. oceanica* has a very large amount of *p*-hydroxybenzoic acid moieties linked to the lignin backbone, which generates phenol upon pyrolysis (Kaal et al., 2016).

3.3.2. THM-GC–MS

The products detected through THM-GC–MS in sediments and macrophytes originated from polysaccharides (e.g. derivatized

metasaccharinic acids), aliphatic compounds (MCC) detected mainly as fatty acid methyl esters (FAMEs), N-compounds (proline and glumatic acid derivatives and dimethylindole), methylated benzene carboxylic acids and a wide range of other methoxybenzenes from polyphenols (Supplementary Table S4).

Among the macrophyte samples analysed, the highest proportions of polysaccharides were detected in *G. barbara* and *C. nodosa* (40–60 %) whereas the lowest proportion of polysaccharides was found in *C. prolifera* (20 %). FAMEs were enriched in *C. prolifera* (40 %), even though the 9/10,16-dimethoxy-C_{16} FAME, which likely originated from cutin in vascular plants, was enriched in *C. nodosa* (12 % vs. <2 % in the other macrophytes). The sum of polyphenol products, that reflects the content of lignin, was the highest in *C. nodosa* (22 %), whereas *G. barbata* and *C. prolifera* showed lower content (4 and 2 %, respectively). The content of phloroglucinols (1,3,5-trimethoxybenzenes) was relevant only in the brown algae *G. barbata* (thus probably indicating phlorotannin) and *C. nodosa* (condensed tannin). Again, α-tocopherol was enriched in *C. prolifera* (7 % vs. <0.5 % in other samples).

The carbohydrate products were depleted in the bare sand core (<3 %), indicating that polysaccharides were scarce probably due to the absence of fresh organic inputs. Furthermore, the benzene carboxylic acid derivative (with two carboxylic groups) was enriched in the samples from the organic matter-depleted bare sand core, indicating insufficiency of diagnostic features for determining the origin of sediment C_{org}. The sum of N-compounds showed a weak correlation with organic matter, but were abundant in the mixed meadow (ranging from 11 to 20 %), variable in macroalgal forests I and II (7–26 % and 5–14 %, respectively), and absent in bare sand. Among the FAMEs, the predominantly cutin-derived product (from leaf cuticles) was enriched in the mixed meadow (20–32 %) and in the macroalgal forest II (5–14 %) and tended to be enriched in organic-rich samples, as well as products of lignin and tannin. It is worth mentioning that by using THM-GC–MS, the polyphenolic pool was not only well-recognized in the sediments from the mixed meadow and macroalgal forest II habitats (as with Py-GC–MS), but also in the macroalgal forest I.

The sum of compounds detected through THM-GC–MS with EF > 3 (Supplementary Table S4) revealed that *C. nodosa* likely contributed most to the sedimentary organic matter across all vegetated habitats, followed by *G. barbata* and *C. prolifera* (Fig. 3). *G. barbata* derived organic matter was identified only in the sediments of the macroalgal forest II and mixed meadow, whereas the results indicated the presence of *C. prolifera* in the sediments of all vegetated habitats.

3.3.3. Stable carbon isotopes

The $\delta^{13}C_{org}$ in the sediments of the macroalgal forests I (−13.7 ± 1.0 ‰) and II (−15.1 ± 0.7 ‰), and the mixed meadow (−13.6 ± 0.2 ‰) were similar, and significantly higher than in the bare sand (−22.3 ± 0.7 ‰) ($p < 0.001$; Table 1A). The $\delta^{13}C_{org}$ significantly varied along the sediment depth profile in all habitats examined, except for the mixed meadow ($p = 0.062$; Table 1B and Fig. 4A). In the bare sand, $\delta^{13}C_{org}$ followed an increasing downcore trend with significantly higher values towards the end of the core. In the macroalgal forest I, $\delta^{13}C_{org}$ was significantly lower within the top 13 cm decompressed (ranging from −16.6 ‰ to −12.6 ‰) than in deeper sediments (ranging from −11.2 to −10.1 ‰). In the macroalgal forest II, $\delta^{13}C_{org}$ in the top 1.5 cm decompressed (ranging from −20.2 to −15.4 ‰) was significantly lower than in the rest of the core (ranging from −16.8 to −13 ‰) ($p < 0.001$).

All the $\delta^{13}C_{org}$ values of the sediments examined, except two, felt within the range of $\delta^{13}C_{org}$ values from the four potential C_{org} sources considered (Fig. 4B), allowing the application of the Isotope Mixing Model (Parnell and Inger, 2016). The contribution of the C_{org} sources to the sedimentary C_{org} pool varied across habitats and along the sediment depth profile of each habitat (Fig. 5 and Supplementary Table S5). The main contributor to sedimentary C_{org} in the bare sand was seston matter (56 ± 6 %). In the mixed meadow, the contributions of the different sources tested remained relatively stable along the sediment depth

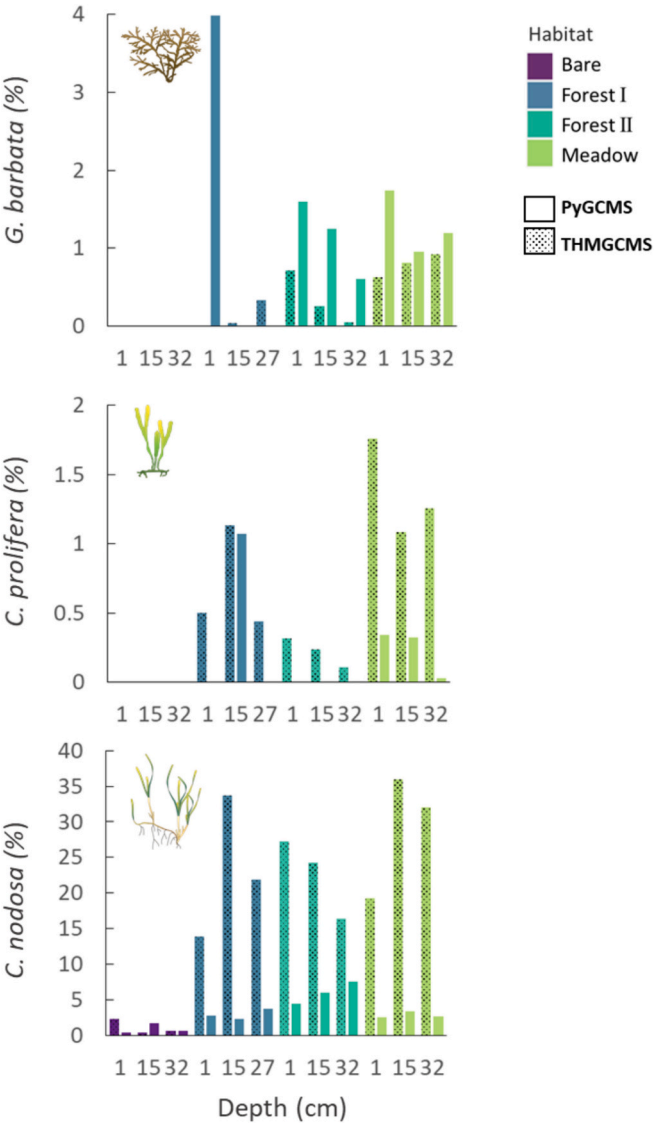

Fig. 3. Py-GC–MS and THM-GC–MS results. Contribution (in %) of *Gongolaria barbata*, *Caulerpa prolifera* and *Cymodocea nodosa* to the sedimentary organic carbon pool at 1 cm, 15 cm and 27/32 cm sediment depths in the bare, macroalgal forest I and II and mixed meadow habitats surveyed. The % contribution was estimated based on the sum of compounds with significant enrichment (EF > 3) for each of the macrophyte species studied.

profile, originating mainly from macroalgae (*C. prolifera*: 33 ± 6 % and *G. barbata*: 18 ± 3 %) and seagrass *C. nodosa* (34 ± 4 %), whereas seston only contributed 15 ± 2 %. Within the top 30 cm sediment of the macroalgal forest I, the contribution of the seagrass *C. nodosa* to the sedimentary C_{org} stock (44 ± 4 %) was similar to that of macroalgae (42 ± 4 %, *G. barbata* and *C. prolifera*), whereas seston accounted for the remaining 14 ± 3 % (Fig. 5). In the macroalgal forest II, the average contribution of the four C_{org} sources examined was similar, ranging from 23 % for both seston and *G. barbata* to 30 % for *C. prolifera*.

4. Discussion

4.1. Magnitude and drivers of sediment C_{org} stocks

Albeit macroalgal ecosystems have been widely overlooked as conceivable carbon reservoirs, this study showcases the potential of Mediterranean macroalgal forests inhabiting sheltered and shallow embayments to store and accumulate carbon in the long-term within and

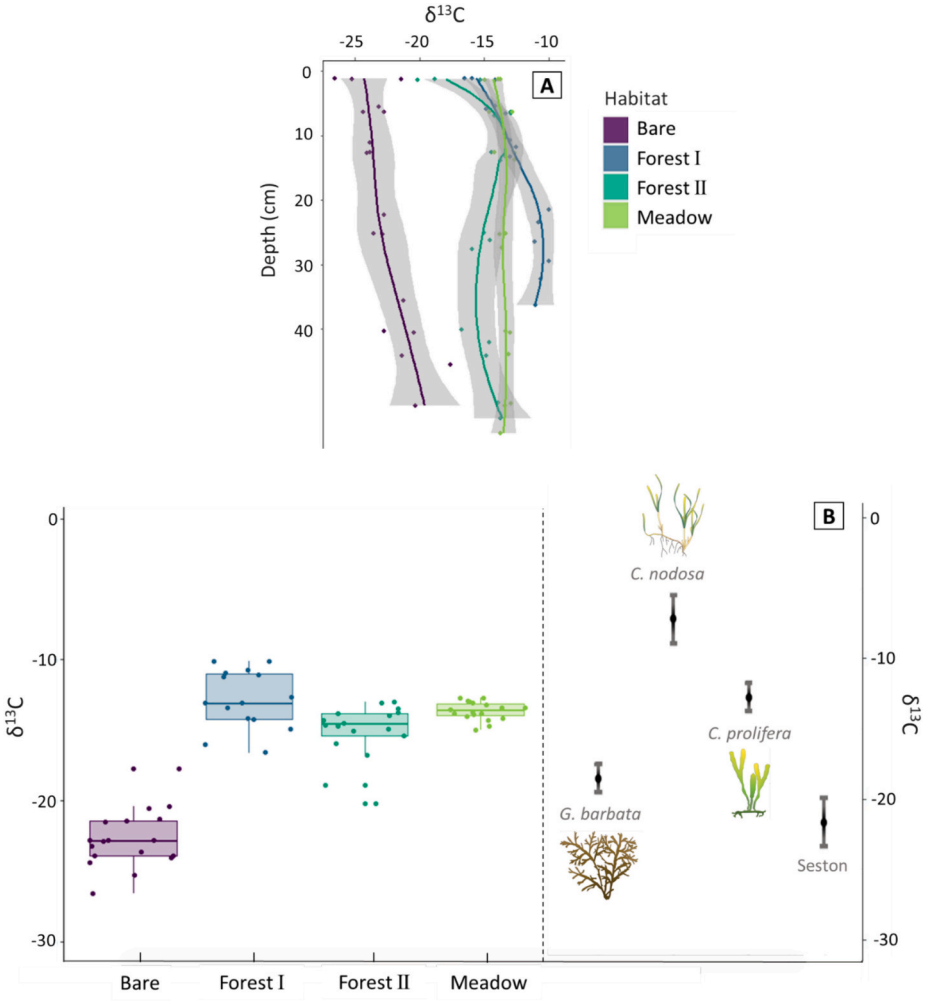

Fig. 4. Stable carbon isotope signatures ($\delta^{13}C_{org}$). A) Downcore trends in sediment $\delta^{13}C_{org}$ values in the three cores studied from each habitat (bare sand, macroalgal forests I and II, and mixed meadow). B) Boxplots showing mean ± SE of $\delta^{13}C_{org}$ values in each habitat, and mean ± SD of $\delta^{13}C_{org}$ values of the potential C_{org} sources (seston, *Caulerpa prolifera*, *Cymodocea nodosa* and *Gongolaria barbata*) to the sedimentary C_{org} pool.

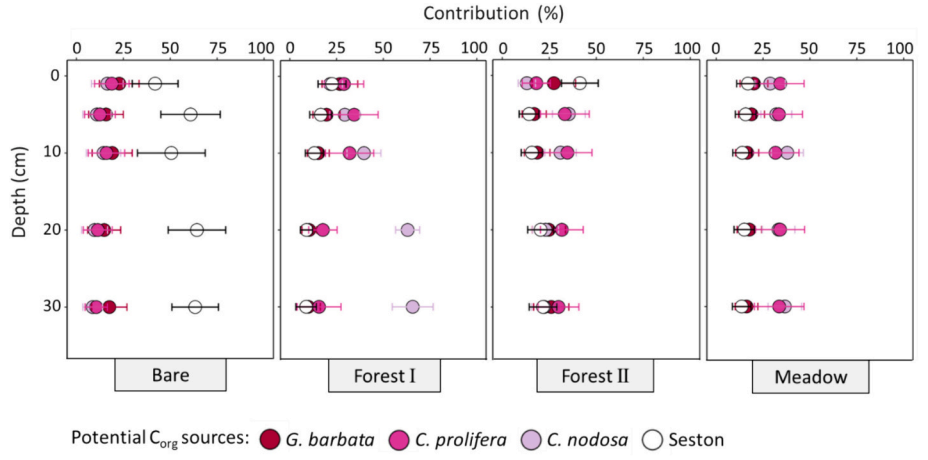

Fig. 5. Bayesian Isotope Mixing Model results along sediment depth in bare, macroalgal forest I and II, and mixed meadow habitats. Proportional contributions (%) of potential sources (*Caulerpa prolifera*, *Cymodocea nodosa*, *Gongolaria barbata* and seston) to the sediment C_{org} pool.

beyond their habitat, supporting the inclusion of this type of macroalgae-dominated ecosystems in Blue Carbon frameworks. In fact, the sediment C_{org} stocks and burial rates found in *G. barbata* forests examined here ranged from 3.2 to 3.8 kg C_{org} m^{-2} and from 12.9 to 18.1 g C_{org} m^{-2} y^{-1} respectively. These values are within the range of those found in *P. oceanica* seagrass meadows for the same region (1.9–11.3 kg C_{org} m^{-2}; Mazarrasa et al., 2017), which is considered a blue carbon outlier among seagrass species due to its large and persistent C_{org} storage

capacity (Fourqurean et al., 2012; Kennedy et al., 2022). Furthermore, both stable carbon isotopes and analytical pyrolysis results showed macroalgae contributions to the sedimentary C_{org} pool of up to approximately 50 % and for up to 70 years.

The magnitude of the sedimentary C_{org} deposits varied across the vegetated habitats examined, likely reflecting differences in structural and biological features of the dominant species, and in the depositional conditions within each habitat (Watanabe et al., 2020). The highest sediment C_{org} stock was found in the mixed *C. prolifera* and *C. nodosa* meadow (4.6 ± 0.3 kg C_{org} m^{-2}), where belowground biomass of these two rhizophytic species directly allocate C_{org} to the soil compartment (Duarte et al., 1998). Moreover, the presence of lignin in *C. nodosa* biomass and its abundance in the sediments of the mixed meadow likely contributed to long-term C_{org} sequestration owing to the relatively high resistance of lignin to microbial degradation under anaerobic conditions (Derenne and Largeau, 2001). Lignin content has been shown to be an important trait driving high soil C_{org} storage in seagrass meadows (Kaal et al., 2020; Kennedy et al., 2022), which together with the substantial C_{org} stores found underneath *C. nodosa* meadows in this and other studies (Bañolas et al., 2020; de los Santos et al., 2023), suggests that this species could be playing a key role in C_{org} storage within shallow water bays in the Mediterranean Sea and Atlantic Ocean (González-García et al., 2022). In fact, according to the stable carbon isotopes, *C. nodosa* was the main source to sedimentary C_{org} in the vegetated habitats examined, contributing between 13 and 67 % to the top 30 cm deposits. The complex root systems of *C. nodosa* and that of the rhizophytic algae *C. prolifera* also contribute to prevent sediment erosion, whereas their dense and continuous canopies enhance the sedimentation and accumulation of particles from the water column (Herkül and Kotta, 2009; Samosorn et al., 2018; de los Santos et al., 2023). This hypothesis is supported by the high silt and clay content (27.0 ± 0.8 %) in the mixed meadow compared to the other studied habitats (ranging from 1.8 to 12.9 %), which likely played a role in the larger C_{org} stocks found in the mixed meadow explaining 23 % of the variability in C_{org} content. In fact, the presence of smaller particle sizes limit oxygen availability and provide protection against remineralization by complexation with organic matter favouring C_{org} preservation in the long-term (Keil et al., 1994; Burdige, 2007). On the contrary, the lowest C_{org} stock found in the bare sand habitat (1.9 ± 0.4 kg C_{org} m^{-2}) could be explained by the coarser nature of the sediment particles, including low silt and clay content (1.8 ± 0.2 %) that reflects a less favourable depositional environment due to the lack of a canopy forming vegetation community. The absence of vegetation in bare sediments entailed that the silt and clay content highly influenced the C_{org} storage (i.e., explaining 51 % of the variability) owing to the limited direct inputs of organic matter from macrophytes, which is reflected by the depletion of carbohydrate products in the sediments of this habitat. The relatively lower sediment C_{org} stocks in the macroalgal forest I compared to the macroalgal forest II could be related to an intense degradation of C_{org} in the former, illustrated by a pronounced decrease of polysaccharides (from Py-GC–MS) at 30 cm sediment depth. In this sense, the lower sedimentation rate in the macroalgal forest I compared to the macroalgal forest II (0.18 ± 0.04 cm y^{-1} and 0.22 ± 0.03 cm y^{-1}, respectively) could have contributed to higher degradation of organic matter upon burial (Serrano et al., 2016). Yet, the high sedimentation rates within the period examined, which may be due to the canopy and the depositional characterises of the sites, fall within the range of sedimentation rates reported for *P. oceanica* in the Mediterranean Sea (0.06–0.41 cm y^{-1}; Duarte et al., 2013), suggesting that they could be an important factor driving the preservation of sedimentary C_{org} in both forests.

4.2. Contribution of macroalgae to sediment C_{org} stocks

Analytical pyrolysis revealed the presence of organic matter derived from the two dominant macroalgae species, *C. prolifera* and *G. barbata*, in the sediments from both macroalgal forests, and in the mixed meadow. The relatively higher contribution of *C. prolifera* to the sedimentary C_{org} pool could be related to its rhizoid and canopy system that, as for seagrasses, facilitates the sedimentation and accumulation of C_{org} in the soil compartment (Hendriks et al., 2010). Indeed, *C. prolifera* is highly productive, and only a few herbivore species can efficiently graze its leaves due to the toxicity of caulerpenyne, the most abundant secondary metabolite of this species (Paul and Fenical, 1987; Sánchez-Moyano et al., 2001). Therefore, most of the plant debris is likely deposited in sediments or exported as detritus. However, the analytical pyrolysis results suggest a decrease in the content of organic matter derived from *C. prolifera* at depths >15 cm, which might reflect rapid remineralization processes upon burial. The long-term carbon sequestration potential of macroalgae is determined by the relative abundance of refractory and labile molecular compounds (Wakeham and Canuel, 2006). The lack of lignin or highly recalcitrant compounds in *C. prolifera*, in accordance with previous studies (Kloareg and Quatrano, 1988), likely renders this species more prone to remineralization compared to *C. nodosa* and thereby, *C. prolifera* has lower potential for long-term burial than seagrasses (Trevathan-Tackett et al., 2015). The decomposition of the more labile OM of *C. prolifera* could trigger the metabolization of *C. nodosa*-derived C_{org} in the mixed meadow by supplementing to the microbial community the energy required for the production of enzymes that degrade recalcitrant compounds (the priming effect) (Trevathan-Tackett et al., 2018). However, this would have been reflected in a decrease in *C. nodosa*-derived C_{org} along depth, which is not the case in the sediments examined. Furthermore, the priming effect is usually promoted by very fast-growing blooming algae that contain even more labile OM than *C. prolifera* (e.g., Ulva spp. Liu et al., 2020). Although recent studies found a low contribution of autochthonous organic matter in sediments under *C. prolifera* meadows (de los Santos et al., 2023), this study suggests that *C. prolifera* might contribute up to 30 % C_{org} to surface C_{org} deposits but due to the low refractory nature of their tissues, its contribution decrease towards deeper and older sedimentary C_{org} stocks.

Despite the lack of belowground biomass and their growth in pebbles on top of sandy substrates, *G. barbata*-derived organic matter contributed between 10 and 27 % C_{org} to the top 30 cm sedimentary deposits in the two macroalgal forests studied. These results contradict previous studies that pointed at a negligible accumulation of macroalgae-derived organic matter in sandy patches between the rocks where they grow (Pessarrodona et al., 2023). In addition, the results showed that *G. barbata* forests can contribute to sediment C_{org} storage in adjacent vegetated habitats, demonstrating that macroalgae contribute to C_{org} storage within and beyond their habitat. In particular, the Isotope Mixing Models suggested that *G. barbata* contributed between 16 and 20 % to the sediment C_{org} deposit in the mixed meadow and between 15 and 24 % at the bare site. However, because of the low amount and highly degraded organic matter in the bare sand, a detailed source assessment through pyrolysis is not sustained, and due to the limitations of stable carbon isotopes to partition the origin of sedimentary C_{org} in coastal settings (Geraldi et al., 2019) caution should be taken with these interpretations. Brown algae usually contain high number of phenols (Hay and Fenical, 1988), and refractory carbon compounds, such as fucoidans (Buck-Wiese et al., 2023) that increase the unpalatability of their biomass and favour their prevalence in sediments. The THM-GC–MS results suggested that the biomass of *G. barbata* is mainly composed of polysaccharides likely related to the alginic acid constituting their cell wall (Manev et al., 2013), but their absence in the sediments suggests that they are probably removed from the tissue as soon as cell structure opens, thereby hindering their long persistence within the sediment (Supplementary Table S4). In fact, in sediments within the macroalgal forest II, the organic molecules derived from *G. barbata* were less detectable with increasing depth, probably due to remineralization of the more labile organic compounds over time (Burdige, 2007). However, the abundance of N-compounds in all depths from the vegetated habitats studied could be linked to contributions of

macroalgae, which are known to have a high nitrogen content. Especially, in the present study, *G. barbata* was the macroalga with the highest N content. On the other hand, the finding of long-chain aliphatic compounds, phenolic compounds, other carbohydrates, and some unidentified compounds in *G. barbata* tissue and in sediment samples (from surface to 30 cm-depth; Supplementary Tables S3 and S4), suggests that these compounds are more persistent to decay. The long-term C_{org} burial potential of *G. barbata* detritus may thus depend on the input of aliphatic and phenolic constituents and the preservation conditions. Further studies are required to unequivocally fingerprint and quantify their contribution.

The relevant contribution of *G. barbata* to sediment C_{org} deposits found in this study can be explained by a combination of biotic and abiotic factors. *G. barbata* exhibits the greatest biomass among the species in the macroalgal forests studied here (Galobart et al., 2023) and therefore, the highest potential for autochthonous C_{org} sequestration (Krumhansl and Scheibling, 2012). Besides, it is a perennial and long-lived species, meaning that its carbon sequestration capacity occurs throughout the whole year. This brown alga contains aerocysts that provide buoyancy and enhance the dispersal of the detached fragments (Riquet et al., 2021). However, individuals growing in Menorca typically display smaller air bladders and in limited quantities (field observation by authors), and in consequence fragments are probably more likely to sink early, either within the habitat itself or in nearby areas. In addition, the calm waters and isolated conditions of the sheltered bays likely favoured macroalgae detritus to sink and bury locally. The relatively high *G. barbata* pool in the mixed meadow (18 ± 3 %), suggests that adjacent vegetated ecosystems play a key role in the sequestration and long-term burial of macroalgae-derived C_{org}. These results showcase the relevance of cross-habitat C_{org} subsides and habitat connectivity for net C_{org} sequestration at a landscape (e.g., embayment) scale (Bulmer et al., 2020) and is consistent with previous studies evidencing that near-shore areas with presence of macroalgal forests close to coastal carbon sinks (including BCE) will likely have a great sequestration potential (Pessarrodona et al., 2023; Ortega et al., 2020; Arina et al., 2023; Hidayah et al., 2022). Therefore, further studies should assess the fate of POC and DOC derived from macroalgal forests and in particular, the portion that can enter long-term sinks including coastal settings and deep-sea ocean waters and sediments (Krause-Jensen and Duarte, 2016).

4.3. Next steps in macroalgal blue carbon research

Currently, most assessments regarding macroalgal blue carbon have focused on the carbon stored in standing living biomass and/or upper sediment layers, that cannot be regarded as permanent reservoirs (Pessarrodona et al., 2023). For example, two recent studies conducted in near-shore locations from Australia (Erlania et al., 2023) and the Arabian Sea (Ortega et al., 2020) demonstrated, through eDNA, the presence of macroalgal in surficial sediments (top ~7 cm). However, these studies hardly trace the contribution of brown algae, which likely constitute the more relevant donors owing to their large biomass and distribution worldwide, due to the limitations of eDNA for this algae group. Indeed, there is a need for validating the export and long-term sequestration of macroalgal carbon in near-shore marine sediments to support their inclusion in climate change mitigation strategies. This study provides compelling evidence of both, with analytical pyrolysis demonstrating the export of macroalgae C_{org} from *G. barbata* forests to adjacent habitats and detecting *G. barbata*-derived organic matter in sediments accumulated for at least the last 70 years. Moreover, the sedimentary C_{org} burial rate of macroalgae within the macroalgal forests examined (calculated from contributions of *G. barbata* and *C. prolifera*) was estimated at 5.4–9.5 g C_{org} m^{-2} y^{-1}, which on average (7.5 ± 2.6 g C_{org} m^{-2} y^{-1}) was 4-fold higher than previous global estimates provided by Krause-Jensen and Duarte (2016) (1.7 ± 0.11 g C_{org} m^{-2} y^{-1}). Yet, further empirical evidence is required across other geographic regions and environmental settings to better understand the contribution of macroalgae forests to sedimentary C_{org} sequestration at a global scale.

4.4. Limitations and caveats

Due to the large temporal and spatial scale, and the complexity of the processes involved in macroalgae C_{org} export and burial, multidisciplinary and intradisciplinary approaches are required to better evaluate and quantify the contribution of macroalgae to the global blue carbon stock in multiple forms (POC, DOC and inorganic carbon) and over large spatial and temporal scales. Here, the synergic and antagonistic results obtained between analytical pyrolysis and Isotope Mixing Models highlight the importance of using a multiproxy approach to contrast and complement information and to better understand the provenance of sedimentary C_{org}. While the combination of bulk $\delta^{13}C$ and Py-GC–MS has been shown to successfully characterize organic matter sources and ecosystem shifts over the past years in seagrass and mangrove environments (Kaal et al., 2020), this approach might not be developed enough to acquire a full picture in blue carbon studies involving macroalgae. One of the main limitations of this study was the use of only three potential macrophyte species as C_{org} donors (also seston in the case of mixing models) probably overestimating their relative contribution to the total carbon pool. An example of this is the presence of debris from *P. oceanica* in the deep layers of the macroalgal forest II that was detected with Py-GC–MS but it was not considered for Isotope Mixing Models since nowadays there is no *P. oceanica* in the study area even though it was probably present before. Including more specific techniques that allow accurate taxonomic discrimination of macrophytes in sediments, such as eDNA or specific biomarkers, will help to expand the list of potential C_{org} sources and to accurately determine the provenance of sediment C_{org}. However, as far as we know, there is no silver bullet available nowadays to accurately identify and quantify the contributors of C_{org} to marine sediments or any other depositional environment.

5. Conclusions

This study provides empirical evidence of the substantial presence of macroalgae-derived C_{org} in sediments accumulated over the past 70 years in the sediments within vegetated habitats in Mediterranean shallow sheltered bays, demonstrating that macroalgal forests play an important role in carbon sequestration and long-term storage, with C_{org} burial and sedimentary stocks comparable to already well-established and recognized BCE. The burial of macroalgae-derived carbon within and beyond their habitat highlights the need to better understand the burial and export pathways of macroalgae-derived organic matter. The fate of C_{org} could be assessed combining traditional isotopic signature and analytical pyrolysis techniques, however, identification of all the potential C_{org} sources with a more accurate taxonomic discrimination will improve this approach. Despite its limitations, this study demonstrates that macroalgae-derived carbon can be stored in coastal shallow settings for long periods of time and thereby, shedding light on the establishment of macroalgae as BCE and their inclusion in climate change mitigation actions. Given their vulnerability to disturbances and their valuable ecosystem services, including blue carbon storage, the health maintenance of macroalgal forests in Mediterranean shallow sheltered bays should be enhanced throughout conservation and restoration initiatives.

CRediT authorship contribution statement

Uxue Moreda: Data curation, Formal analysis, Investigation, Visualization, Writing – original draft. **Inés Mazarrasa:** Investigation, Supervision, Validation, Writing – review & editing. **Emma Cebrian:** Conceptualization, Funding acquisition, Project administration, Supervision, Writing – review & editing. **Joeri Kaal:** Data curation, Formal analysis, Investigation, Writing – review & editing. **Aurora M. Ricart:**

Investigation, Writing – review & editing. **Eduard Serrano:** Investigation, Writing – review & editing. **Oscar Serrano:** Conceptualization, Funding acquisition, Project administration, Supervision, Writing – review & editing.

Declaration of competing interest

The authors declare that they have no known competing financial interests or personal relationships that could have appeared to influence the work reported in this paper.

Data availability

Data will be made available on request.

Acknowledgements

Authors acknowledge the D.G. d'Espais Naturals i Biodiversitat, the D.G. de Pesca i Medi Marí, and the Servei en Recerca i Desenvolupament del Govern de les Illes Balears for providing licenses, and the Jaume Ferrer Marine Station (IEO) for technical and facility support. Thanks to Peter G. Appleby from the Environmental Radioactivity Research Centre in the University of Liverpool and to the Support services for research (SAI) of the University of A Coruña for assistance with laboratory and analytical procedures.

Funding

O.S. was supported by I + D + i projects RYC2019-027073-I and PIE HOLOCENO 20213AT014 funded by MCIN/AEI/10.13039/501100011033 and FEDER. E.C. research was funded by the following projects: 1) the European Union – NextGeneration EU – as part of the MITECO program for the Spanish Recovery, Transformation and Resilience Plan (Recovery and Resilience Facility of the European Union established by the Regulation (EU) 2020/2094), and was entrusted to CSIC, AZTI, SOCIB, and the universities of Vigo and Cadiz; 2) The Spanish Ministry of Science and Innovation under the grant FORESTA - N° PID2020-112985GB-I00, funded by MCIN/AEI/10.13039/501100011033 (European Union). U.M. was funded by The Spanish Ministry of Science and Innovation under the fellowship JAE Intro 2023 JAEINT23_EX_0605. I.M. was supported by a Juan de la Cierva Incorporación postdoctoral fellowship of the Spanish Ministry of Science and Innovation JC2020-045917-I. A.M.R was supported by project PCI2021-122040-2B funded by MCIN/AEI/10.13039/501100011033 and the European Union – NextGeneration EU/Recovery, Transformation and Resilience Plan.

Appendix A. Supplementary data

Supplementary data to this article can be found online at https://doi.org/10.1016/j.scitotenv.2024.173219.

References

Ager, T.G., Krause-Jensen, D., Olesen, B., Carlson, D.F., Winding, M.H.S., Sejr, M.K., 2023. Macroalgal habitats support a sustained flux of floating biomass but limited carbon export beyond a Greenland fjord. Sci. Total Environ. 872, 162224.

Appleby, P.G., Nolan, P.J., Gifford, D.W., Godfrey, M.J., Oldfield, F.J.A.N., Anderson, N. J., Battarbee, R.W., 1986. 210 Pb dating by low background gamma counting. Hydrobiologia 143, 21–27.

Appleby, P.G., Richardson, N., Nolan, P.J., 1992. Self-absorption corrections for well-type germanium detectors. Nucl. Instrum. Methods Phys. Res., Sect. B 71 (2), 228–233.

Arina, N., Hidayah, N., Hazrin-Chong, N.H., Rozaimi, M., 2023. Algal contribution to organic carbon sequestration and its signatures in a tropical seagrass meadow. Deep Sea Res. Part II: Top. Stud. Oceanogr. 210, 105307.

Bañolas, G., Fernández, S., Espino, F., Haroun, R., Tuya, F., 2020. Evaluation of carbon sinks by the seagrass *Cymodocea nodosa* at an oceanic island: spatial variation and economic valuation. Ocean Coast. Manag. 187, 105112.

Bates, D., Mächler, M., Bolker, B., Walker, S., 2015. Fitting linear mixed-effects models using lme4. J. Stat. Softw. 67 (1), 1–48.

Buck-Wiese, H., Andskog, M.A., Nguyen, N.P., Bligh, M., Asmala, E., Vidal-Melgosa, S., Hehemann, J.H., 2023. Fucoid brown algae inject fucoidan carbon into the ocean. Proc. Natl. Acad. Sci. 120 (1).

Bulmer, R.H., Stephenson, F., Jones, H.F., Townsend, M., Hillman, J.R., Schwendenmann, L., Lundquist, C.J., 2020. Blue carbon stocks and cross-habitat subsidies. Front. Mar. Sci 380.

Burdige, D.J., 2007. Preservation of organic matter in marine sediments: controls, mechanisms, and an imbalance in sediment organic carbon budgets? Chem. Rev. 107 (2), 467–485.

Claes, J., Hopman, D., Jaeger, G., Rogers, M., 2022. Blue Carbon: The Potential of Coastal and Oceanic Climate Action. McKinsey & Company, Hong Kong, China.

Dauby, P., 1989. The stable carbon isotope ratios in benthic food webs of the Gulf of Calvi, Corsica. Continental Shelf Res. 9 (2), 181–195.

de los Santos, C.B., Egea, L.G., Martins, M., Santos, R., Masqué, P., Peralta, G., Jiménez-Ramos, R., 2023. Sedimentary organic carbon and nitrogen sequestration across a vertical gradient on a temperate wetland seascape including salt marshes, seagrass meadows and rhizophytic macroalgae beds. Ecosystems 26, 1–17.

Derenne, S., Largeau, C., 2001. A review of some important families of refractory macromolecules: composition, origin, and fate in soils and sediments. Soil Sci. 166 (11), 833–847.

Derrien, M., Yang, L., Hur, J., 2017. Lipid biomarkers and spectroscopic indices for identifying organic matter sources in aquatic environments: a review. Water Res. 112, 58–71.

Duarte, C.M., Merino, M., Agawin, N.S., Uri, J., Fortes, M.D., Gallegos, M.E., Hemminga, M.A., 1998. Root production and belowground seagrass biomass. Mar. Ecol. Prog. Ser. 171, 97–108.

Duarte, C.M., Kennedy, H., Marbà, N., Hendriks, I., 2013. Assessing the capacity of seagrass meadows for carbon burial: current limitations and future strategies. Ocean Coast. Manag. 83, 32–38.

Duarte, C.M., Gattuso, J.P., Hancke, K., Gundersen, H., Filbee-Dexter, K., Pedersen, M.F., Krause-Jensen, D., 2022. Global estimates of the extent and production of macroalgal forests. Glob. Ecol. Biogeogr. 31 (7), 1422–1439.

Erlania, E., Bellgrove, A., Macreadie, P.I., Young, M.A., Holland, O.J., Clark, Z., Miller, A. D., 2023. Patterns and drivers of macroalgal 'blue carbon' transport and deposition in near-shore coastal environments. Sci. Total Environ. 890, 164430.

Evershed, R.P., Bull, I.D., Corr, L.T., Crossman, Z.M., van Dongen, B.E., Evans, C.J., Pancost, R.D., 2007. Compound-specific stable isotope analysis in ecology and paleoecology. In: Stable Isotopes in Ecology and Environmental Science, 480.

Filbee-Dexter, K., Wernberg, T., 2018. Rise of turfs: a new battlefront for globally declining kelp forests. Bioscience 68 (2), 64–76.

Fourqurean, J.W., Marbà, N., Duarte, C.M., Díaz-Almela, E., Ruiz-Halpern, S., 2007. Spatial and temporal variation in the elemental and stable isotopic content of the seagrasses *Posidonia oceanica* and *Cymodocea nodosa* from the Illes Balears, Spain. Mar. Biol. 151, 219–232.

Fourqurean, J.W., Duarte, C.M., Kennedy, H., Marbà, N., Holmer, M., Mateo, M.A., Serrano, O., 2012. Seagrass ecosystems as a globally significant carbon stock. Nat. Geosci. 5 (7), 505–509.

Galobart, C., Ballesteros, E., Golo, R., Cebrian, E., 2023. Addressing marine restoration success: evidence of species and functional diversity recovery in a ten-year restored macroalgal forest. Front. Mar. Sci. 10, 1176655.

Gattuso, J.P., Magnan, A.K., Bopp, L., Cheung, W.W., Duarte, C.M., Hinkel, J., Rau, G.H., 2018. Ocean solutions to address climate change and its effects on marine ecosystems. Front. Mar. Sci. 337.

Geraldi, N.R., Ortega, A., Serrano, O., Macreadie, P.I., Lovelock, C.E., Krause-Jensen, D., Duarte, C.M., 2019. Fingerprinting blue carbon: rationale and tools to determine the source of organic carbon in marine depositional environments. Front. Mar. Sci. 263.

González-García, A., Arias, M., García-Tiscar, S., Alcorlo, P., Santos-Martín, F., 2022. National blue carbon assessment in Spain using InVEST: current state and future perspectives. Ecosyst. Serv. 53, 101397.

Govan, E., Parnell, A., 2019. simmr: A Stable Isotope Mixing Model. R package version 0.5.1.216. https://CRAN.R-project.org/package=simmr.

Gruber, R.K., Kemp, W.M., 2010. Feedback effects in a coastal canopy-forming submersed plant bed. Limnol. Oceanogr. 55 (6), 2285–2298.

Handayani, T., Zulpikar, F., Kusnadi, A., 2022. The roles of macroalgae in climate change mitigation: opportunities and challenges for marine-based carbon donor. IOP Conf. Ser. Earth Environ. Sci. 1119 (1), 012014.

Hay, M.E., Fenical, W., 1988. Marine plant-herbivore interactions: the ecology of chemical defense. Annu. Rev. Ecol. Syst. 19 (1), 111–145.

Heiri, O., Lotter, A.F., Lemcke, G., 2001. Loss on ignition as a method for estimating organic and carbonate content in sediments: reproducibility and comparability of results. J. Paleolimnol. 25, 101–110.

Hendriks, I.E., Bouma, T.J., Morris, E.P., Duarte, C.M., 2010. Effects of seagrasses and algae of the Caulerpa family on hydrodynamics and particle-trapping rates. Mar. Biol. 157, 473–481.

Herkül, K., Kotta, J., 2009. Effects of eelgrass (*Zostera marina*) canopy removal and sediment addition on sediment characteristics and benthic communities in the Northern Baltic Sea. Mar. Ecol. 30, 74–82.

Hidayah, N., Ng, C.T., Arina, N., Fairoz, M., Rozaimi, M., 2022. Macroalgal and mangrove provenances demonstrate their relevance in contributing to the blue carbon pool of a tropical seagrass meadow. Ecol. Res. 37 (1), 21–32.

Himes-Cornell, A., Pendleton, L., Atiyah, P., 2018. Valuing ecosystem services from blue forests: a systematic review of the valuation of salt marshes, sea grass beds and mangrove forests. Ecosyst. Serv. 30, 36–48.

Kaal, J., Serrano, O., Nierop, K.G., Schellekens, J., Cortizas, A.M., Mateo, M.Á., 2016. Molecular composition of plant parts and sediment organic matter in a Mediterranean seagrass (Posidonia oceanica) mat. Aquat. Bot. 133, 50–61.
Kaal, J., Cortizas, A.M., Mateo, M.Á., Serrano, O., 2020. Deciphering organic matter sources and ecological shifts in blue carbon ecosystems based on molecular fingerprinting. Sci. Total Environ. 742, 140554.
Keil, R.G., Montluçon, D.B., Prahl, F.G., Hedges, J.I., 1994. Sorptive preservation of labile organic matter in marine sediments. Nature 370 (6490), 549–552.
Kennedy, H., Beggins, J., Duarte, C.M., Fourqurean, J.W., Holmer, M., Marbà, N., Middelburg, J.J., 2010. Seagrass sediments as a global carbon sink: isotopic constraints. Global Biogeochem. Cycles 24 (4).
Kennedy, H., Pagès, J.F., Lagomasino, D., Arias-Ortiz, A., Colarusso, P., Fourqurean, J. W., Duarte, C.M., 2022. Species traits and geomorphic setting as drivers of global soil carbon stocks in seagrass meadows. Global Biogeochem. Cycles 36 (10).
Kloareg, B., Quatrano, R.S., 1988. Structure of the cell walls of marine algae and ecophysiological functions of the matrix polysaccharides. Oceanogr. Mar. Biol. Annu. Rev. 26, 259–315.
Krause-Jensen, D., Duarte, C.M., 2016. Substantial role of macroalgae in marine carbon sequestration. Nat. Geosci. 9 (10), 737–742.
Krishnaswamy, S., Lal, D., Martin, J.M., Meybeck, M., 1971. Geochronology of lake sediments. Earth Planet. Sci. Lett. 11 (1–5), 407–414.
Krumhansl, K.A., Scheibling, R.E., 2012. Production and fate of kelp detritus. Mar. Ecol. Prog. Ser. 467, 281–302.
Liu, S., Trevathan-Tackett, S.M., Ewers Lewis, C.J., Huang, X., Macreadie, P.I., 2020. Macroalgal blooms trigger the breakdown of seagrass blue carbon. Environ. Sci. Technol. 54 (22), 14750–14760.
Lovelock, C.E., Reef, R., 2020. Variable impacts of climate change on blue carbon. One Earth 3 (2), 195–211.
Macreadie, P.I., Costa, M.D., Atwood, T.B., Friess, D.A., Kelleway, J.J., Kennedy, H., Duarte, C.M., 2021. Blue carbon as a natural climate solution. Nat. Rev. Earth Environ. 2 (12), 826–839.
Manev, Z., Iliev, A., Vachkova, V., 2013. Chemical characterization of brown seaweed—Cystoseira barbata. Bulgarian J. Agr. Sci. 19 (1), 12–15.
Mateo, M.A., Romero, J., Pérez, M., Littler, M.M., Littler, D.S., 1997. Dynamics of millenary organic deposits resulting from the growth of the Mediterranean seagrass *Posidonia oceanica*. Estuar. Coast. Shelf Sci. 44 (1), 103–110.
Mazarrasa, I., Marbà, N., Garcia-Orellana, J., Masqué, P., Arias-Ortiz, A., Duarte, C.M., 2017. Effect of environmental factors (wave exposure and depth) and anthropogenic pressure in the C sink capacity of *Posidonia oceanica* meadows. Limnol. Oceanogr. 62 (4), 1436–1450.
Mcleod, E., Chmura, G.L., Bouillon, S., Salm, R., Björk, M., Duarte, C.M., Silliman, B.R., 2011. A blueprint for blue carbon: toward an improved understanding of the role of vegetated coastal habitats in sequestering CO_2. Front. Ecol. Environ. 9 (10), 552–560.
Novoa, E.A.M., Guiry, M.D., 2019. Reinstatement of the genera *Gongolaria* Boehmer and *Ericaria* Stackhouse (Sargassaceae, Phaeophyceae). Eur. J. Phycol. 54 (3), 456.
Ortega, A., Geraldi, N.R., Duarte, C.M., 2020. Environmental DNA identifies marine macrophyte contributions to blue carbon sediments. Limnol. Oceanogr. 65 (12), 3139–3149.
Papadimitriou, S., Kennedy, H., Kennedy, D.P., Duarte, C.M., Marbà, N., 2005. Sources of organic matter in seagrass-colonized sediments: a stable isotope study of the silt and clay fraction from *Posidonia oceanica* meadows in the western Mediterranean. Org. Geochem. 36 (6), 949–961.
Parnell, A., Inger, R., 2016. Simmr: A Stable Isotope Mixing Model. R package version 0.3. R.
Paul, V.J., Fenical, W., 1987. Natural products chemistry and chemical defense in tropical marine algae of the phylum Chlorophyta. Bioorganic Mar. Chem. 1–29.
Pessarrodona, A., Filbee-Dexter, K., Alcoverro, T., Boada, J., Feehan, C.J., Fredriksen, S., Wernberg, T., 2021. Homogenization and miniaturization of habitat structure in temperate marine forests. Glob. Chang. Biol. 27 (20), 5262–5275.
Pessarrodona, A., Franco-Santos, R.M., Wright, L.S., Vanderklift, M.A., Howard, J., Pidgeon, E., Filbee-Dexter, K., 2023. Carbon sequestration and climate change mitigation using macroalgae: a state of knowledge review. Biol 98, 1945–1971.
Pulchan, J., Abrajano, T.A., Helleur, R., 1997. Characterization of tetramethylammonium hydroxide thermochemolysis products of near-shore marine sediments using gas chromatography/mass spectrometry and gas chromatography/combustion/isotope ratio mass spectrometry. J. Anal. Appl. Pyrolysis 42 (2), 135–150.
Queirós, A.M., Stephens, N., Widdicombe, S., Tait, K., McCoy, S.J., Ingels, J., Somerfield, P.J., 2019. Connected macroalgal-sediment systems: blue carbon and food webs in the deep coastal ocean. Ecological monographs 89 (3), e01366.
Queirós, A.M., Tait, K., Clark, J.R., Bedington, M., Pascoe, C., Torres, R., Smale, D.A., 2023. Identifying and protecting macroalgae detritus sinks toward climate change mitigation. Ecol. Appl. 33 (3), e2798.
R Core Team, 2023. R: A Language and Environment for Statistical Computing. R Foundation for Statistical Computing, Vienna, Austria. https://www.R-project.org/.
Reef, R., Atwood, T.B., Samper-Villarreal, J., Adame, M.F., Sampayo, E.M., Lovelock, C. E., 2017. Using eDNA to determine the source of organic carbon in seagrass meadows. Limnol. Oceanogr. 62 (3), 1254–1265.
Riquet, F., De Kuyper, C.A., Fauvelot, C., Airoldi, L., Planes, S., Fraschetti, S., Bottin, L., 2021. Highly restricted dispersal in habitat-forming seaweed may impede natural recovery of disturbed populations. Sci. Rep. 11 (1), 16792.
Samosorn, S., Sangtiean, T., Rodtassana, C., Poungparn, S., 2018. Roles of aboveground roots facilitating sedimentation and elevation change in a mangrove forest behind bamboo seawalls. Songklanakarin J. Sci. Technol. 40, 1315–1323.
Sánchez-Moyano, J.E., Estacio, F.J., García-Adiego, E.M., García-Gómez, J.C., 2001. Effect of the vegetative cycle of *Caulerpa prolifera* on the spatio-temporal variation of invertebrate macrofauna. Aquat. Bot. 70 (2), 163–174.
Sarà, G., Vizzini, S., Mazzola, A., 2003. Sources of carbon and dietary habits of new Lessepsian entry *Brachidontes pharaonis* (Bivalvia, Mytilidae) in the western Mediterranean. Mar. Biol. 143, 713–722.
Serrano, O., Lavery, P.S., Rozaimi, M., Mateo, M.Á., 2014. Influence of water depth on the carbon sequestration capacity of seagrasses. Global Biogeochem. Cycles 28 (9), 950–961.
Serrano, O., Ricart, A.M., Lavery, P.S., Mateo, M.A., Arias-Ortiz, A., Masque, P., Duarte, C.M., 2016. Key biogeochemical factors affecting soil carbon storage in *Posidonia* meadows. Biogeosciences 13 (15), 4581–4594.
Smith, S.V., 1981. Marine macrophytes as a global carbon sink. Science 211 (4484), 838–840.
Thibaut, T., Pinedo, S., Torras, X., Ballesteros, E., 2005. Long-term decline of the populations of Fucales (*Cystoseira* spp. and *Sargassum* spp.) in the Albères coast (France, North-western Mediterranean). Mar. Pollut. Bull. 50 (12), 1472–1489.
Trevathan-Tackett, S.M., Kelleway, J., Macreadie, P.I., Beardall, J., Ralph, P., Bellgrove, A., 2015. Comparison of marine macrophytes for their contributions to blue carbon sequestration. Ecology 96 (11), 3043–3057.
Trevathan-Tackett, S.M., Thomson, A.C., Ralph, P.J., Macreadie, P.I., 2018. Fresh carbon inputs to seagrass sediments induce variable microbial priming responses. Sci. Total Environ. 621, 663–669.
Van de Meent, D., de Leeuw, J.W., Schenck, P.A., 1980. Chemical characterization of nonvolatile organics in suspended matter and sediments of the river Rhine Delta. J. Anal. Appl. Pyrolysis 2, 249–263.
Vizzini, S., Sarà, G., Michener, R.H., Mazzola, A.J.A.O., 2002. The role and contribution of the seagrass *Posidonia oceanica* (L.) Delile organic matter for secondary consumers as revealed by carbon and nitrogen stable isotope analysis. Acta Oecol. 23 (4), 277–285.
Wakeham, S.G., Canuel, E.A., 2006. Degradation and preservation of organic matter in marine sediments. In: Marine Organic Matter: Biomarkers, Isotopes and DNA, pp. 295–321.
Watanabe, K., Yoshida, G., Hori, M., Umezawa, Y., Moki, H., Kuwae, T., 2020. Macroalgal metabolism and lateral carbon flows can create significant carbon sinks. Biogeosciences 17 (9), 2425–2440.